NEAR IR ANALYSIS IN THE PROBLEMATIC HIGHLY CONCENTRATED DOMAIN

Stuart Licht* and Alexey Heiman

Department of Chemistry
Technion – Israel Institute of Technology
Haifa, 32000, Israel

SUMMARY

Solution phase methodologies have focused on analysis of dilute solutions for both pragmatic and fundamental reasons. Yet, in industrial, environmental and many synthetic and research processes, highly concentrated solutions are prevalent. Dilution steps can lengthen analysis time, add contaminants, and lead to the disregard of interesting complexation, association, or solvent driven equilibria which can occur only in the concentrated phase. We have developed and presented a variety of novel methodologies which are suitable for direct analysis of concentrated solutions. The methodologies are entitled: Evanescent (Solvent) Activity Analysis, Concentrated Solution Potentiometric and Near IR Analysis, Differential Conductometric Analysis, Differential Densometric Analysis, and Sub-Micron Path UV/VIS/IR Spectroscopy. In this study we focus on Near IR Analysis in the Problematic Highly Concentrated Domain. At 967 or 1421 nm a (hydroxide) absorption peak increases smoothly with increasing hydroxide activity. Second-order differentiation, $\partial^2 A/\partial l^2$, at either 967 or 1421 nm, minimizes the effects of the nearby bulk water absorption, and of baseline shift, and provides a linear variation with hydroxide concentration.

Keywords:
Near Infrared Spectroscopy; Absorption spectroscopy; Hydroxide analysis; Concentrated solution analysis.

---

* Author to whom correspondence should be addressed.

INTRODUCTION

In industrial, environmental and many synthetic and research processes, highly concentrated solutions are prevalent. Dilution steps can lengthen analysis time, add contaminants, and lead to the disregard of interesting complexation, association, or solvent driven equilibria which can occur only in the concentration phase. We have developed and presented a variety of novel methodologies which are suitable for direct analysis of concentrated solutions. The methodologies are entitled: Evanescent (Solvent) Activity Analysis, Concentrated Solution Potentiometric and Near IR Analysis, Differential Conductometric Analysis, Differential Densometric Analysis, and Sub-Micron Path UV/VIS/IR Spectroscopy. In this study we focus on Near IR Analysis in the Problematic Highly Concentrated Domain.

Although it is the most widely studied solvent, considerable uncertainty remains over the fundamental structure of simple water /1/. For example, new evidence for a structure principally governed by a six or eight member molecule cage of water has been presented in the past few years, and despite more than a century of studies, interpretations based on the accumulated evidence still seem to change on an annual basis /1-5/. This uncertainty in water's microscopic properties and structure affects the assignment of the spectroscopic bands of water in the Near Infrared (NIR) region. The principal feature of the water spectrum in the range of 900-1700 nm is a peak at approximately 1460 nm with a path length normalized absorbance of A = 14 cm^{-1}. This absorption peak has to be assigned to the combination transition $\nu_1 + \nu_3$, where ν_1 is the symmetric stretch, and ν is the antisymmetric stretch of a water molecule /6/. Other significant features of the water NIR spectrum are bands centered at approximately 976 and 1200 nm. At these wavelengths, maximum absorption values of A = 0.24 cm^{-1} and 0.53 cm^{-1} respectively occur in pure water. These absorption bands have been assigned to the combination transitions $2\nu_1 + \nu_3$, and $\nu_1 + \nu_2 + \nu_3$, where ν_2 is a bending vibration for the water molecule /6/. However, the accumulating evidence of the water microstructure suggests that this interpretation is considerably over-simplified, leading to uncertainties in the spectral assignments /6-9/. The difficulty in obtaining a rigorous molecular-scale description of water structure is largely a consequence of the extended hydrogen-bonded network that exists throughout the liquid /1/. This network and these interactions will be considerably affected by concentrated analytes. From an analytical perspective, the fundamental nature of these interactions is less important

than their influence on analyte determinations, and as will be shown in this study this influence can be substantial.

Distinctive, relatively small, analyte extinction coefficients in the NIR region have led to NIR methodologies widely suggested to probe the composition of concentrated solutions. Spectroscopic bands in this region, which are assigned to overtones and combination modes of fundamental vibrations, do not usually have high extinction coefficients. Therefore this spectroscopic range is suitable for analysis of concentrated solutions. Near-infrared spectral analysis has been proposed for the determination of salinity /10/. Lin and Brown /11/, by means of investigation of aqueous solutions between 1100 and 1900 nm, studied seawater and up to 5 **m** NaCl, to show that near-infrared spectroscopy could be used in the determination of a variety of physical/chemical properties. Watson and Baughman /12/ explored near-infrared spectroscopy of hydroxide ions up to concentrations of 2.5 **m** NaOH in the region 1000 to 2500 nm. NIR spectroscopy is appropriate for non-invasive multi-component analysis of a variety of co-existing species. The quantitative analysis of solutions containing various concentrations of NaOH, NaCl, and Na_2CO_3, up to 2.5 **m**, was investigated by Grant *et al.* /13/ at 1440 and 1930 nm. Similarly, investigators have used NIR to probe high concentrations of HF /14/, oxygenates /15/, alcohols /16/, humidity /17/, and multicomponent species /18-20/.

The new NIR methodologies are of significant importance due to limitations in other conventional solution phase methodologies. Analyte concentrations of 0.1 **m** and higher prevail in many environmental, research and industrial systems. Analyte dilution to provide compatibility with conventional analytical methodologies impedes real-time analysis, and also precludes determination of individual species in concentrated solution (speciation). There are few analytical methodologies available to probe the *in-situ* analysis of concentrated solutions, which often take advantage of physical/chemical properties which are accentuated, rather than obscured, in highly concentrated media /21-26/. A principal limitation of conventional absorption spectroscopy is the inability to discern concentrated analytes. Indeed, most analytical methods focused on millimolal or lower analyte concentrations. For example, excessive liquid junction potentials are expected in the electroanalysis of concentrated analytes. Similarly, conventional analyte extinction coefficients lead to excessive spectral absorption at molar level concentration of analytes. In addition to excessive absorption, traditional challenges to spectroscopic analysis of the concentrated domain

include excessive absorption, solvent effects, variation of index of refraction, as well as problematic analysis due to peak displacement and broad band absorption. The substantial deviation from unit activity coefficient complicates analysis of colorimetric indicators. Each effect obscures traditional Beer-Lambert analysis /24,27,28/.

As a non-invasive technique, specific weak absorptions which occur in the near-infrared region may permit analysis of concentrated solutions /29/. However, problems related to using aqueous IR spectroscopy include the tendency for strong overlap of significant solvent and solute spectral features, and uncertainty of interferant effects /30/. They require adapted methods of analysis. In this study, as exemplified by alkaline hydroxide solutions, it is shown that analyte strongly affects the conventional aqueous baseline of these measurements, and this baseline behavior must be addressed for effective NIR analysis. In the domain of molal analyte concentrations, the water baseline changes drastically as solute can bind and confine bulk solvent. Recognition of these variations permits an effective NIR determination of analytes (in this case hydroxide).

EXPERIMENTAL SECTION

All solutions described were prepared with analytical grade reagents dissolved in double deionized (D4727 NANOpure Analytical Deionization System) water. Saturated stock solutions were prepared, filtered, and standardized by titration with Normex 1 M HCl Fixanal by Carlo Erba Reagenti. From these stock solutions, solutions with lower concentrations were prepared. The solutions were left quiescent for sufficient time (in the order of hours; time required increases with solution viscosity) to remove air bubbles that otherwise cause severe baseline shift. Concentrated solutions generally are reported in molal (mass based), rather than molar (volume based) units to probe thermodynamic activities, and molal concentration units are used throughout this study. However, despite the lower precision of volume based molar units, they still find widespread use. Therefore molar units are included in the final section of the study, and are derived from the conventional conversion $\mathbf{M} = d/(Mw + \mathbf{m}^{-1})$, where Mw is the molecular weight of the solute, d(kg/liter) is the solution density, and molarity and molality have units of **M** (moles/liter) and **m** (moles/kg solvent).

Absorption spectra were measured with either of two instruments, UV/Visible and short NIR wavelengths (in the range of 190-1100 nm) spectra were probed with an HP 8453 UV-Visible Photodiode Array Spectrophotometer at a temperature T = 20 ± 1°C. Samples in the above range were measured in a quartz cuvette with 1.00-cm path lengths. All spectra are the result of an averaging of 100 scans, and HP UV-Visible ChemStation Software was used to calculate second-order derivative spectra, applying the Savitsky-Golay algorithm. Absorption spectra in the range of 900-1300 and 1100-1700 nm were measured using an ORIEL tungsten-halogen lamp illumination source, and an Acton Research Corporation Spectra pro-275 spectrometer with a germanium detector. The data were acquired by means of a lock-in amplifier. Samples in the ranges of 900-1300 and 1100-1700 nm were measured in a quartz cuvette with 1.00-cm and 0.5-mm path length, respectively.

RESULTS AND DISCUSSION

Baseline variations

Figure 1 and the figure inset demonstrate changes occurring in the NIR spectra of NaOH solutions in the range from 900-1700 nm. Short-wave NIR spectra were measured and analyzed for a range of concentrations up to saturation, and for a variety of alkaline solutions (LiOH, NaOH, KOH, CsOH). The resurgence of interest in the NIR region is a relatively new phenomenon and NIR spectra of concentrated LiOH, KOH and CsOH electrolytes have not been previously reported, nor have NIR spectra of over 5 molal NaOH. In these solutions, the spectroscopic bands in the 900-1700 nm region are related to the substantial overlapping of overtones and combinations from fundamental modes of O–H vibrations. As will be shown, these near-infrared spectroscopic bands are considerably influenced by speciation of solutions, solute concentration, and the bulk properties of water. These properties also vary with solution composition, and, as exemplified by water activity which can diminish by more than an order of magnitude in concentrated aqueous solutions, these properties are expected to change drastically in concentrated solutions. Hence, any spectroscopic measurements in this spectral range (900-1700 nm) and concentration range (1 molal solute and up) which are computed from the difference to an invariant solvent blank will lead to substantial errors in solute analysis. However, as will be

demonstrated, recognition of these baseline variations can lead to effective and useful analyte determination in this spectral and concentration domain.

Spectroscopic assignment

Figure 1 and its inset present the spectra of a wide range of NaOH concentrations referenced to air in the range of 900-1700 nm. The main feature of the water spectrum in the range of 1300-1700 nm is a broad peak at 1450 nm of path length normalized absorption, A = 14 cm^{-1} pathlength. However, as seen in the figure at high concentrations, an additional peak is evident at 1420 nm with increasing free hydroxide concentration, and it is correlated with the first overtone of free hydroxide. At these higher hydroxide concentrations, as known water activity decreases, the ~1450 nm band associated with the $\nu_1 + \nu_3$ combination stretch band in bulk water is seen to decrease and appears to shift to longer wavelengths (from approximately 1457 to 1465 nm), but further analysis of this shift is problematic due to the effect of nearby large absorptions occurring at both longer and shorter wavelengths. The water activity, a_w, in these concentrated electrolytes has been well characterized /31/, and the decrease from a_w (pure water) = 1, to a_w (7.0 **m** NaOH) = 0.67, to a_w (27 **m** NaOH) = 0.07, is reflected in a variety of properties including the observed decrease in water vapor pressure above these solutions /21,24/ and redox potential variations /26/. Water activity diminishes when a significant fraction of the 55.5 **m** bulk water in the pure solvent is increasingly bound within the hydration sphere of the concentrated solute. The absorbance at 1457 nm exhibits a linear decrease with decreasing availability of bulk water (water activity). It has been suggested that the peak arising at 1421 nm is due to the first overtone of the O–H stretching mode /32/, and as seen in Figure 1, the use of highly concentrated alkaline electrolytes permits this peak to be sharply defined.

As seen in the Figure 1 inset, in the range of 900-1300 nm, the principal features of the water spectrum are bands centered at 976 and 1199 nm. At this wavelength, the maximum path length normalized absorption values of A (976 nm) = 0.24 cm^{-1} and A (1199 nm) = 0.53 cm^{-1}, respectively, occur in pure water. The broad series of peaks centered at 1199 nm, and ranging from 1080 to 1250 nm, consistently decrease with increasing NaOH concentration. Hence, the spectral bands in this region all decrease with decreasing water activity. The concentration variation of the peaks centered at 976 in pure water is more complex (Fig. 2). The inset of Figure 2 shows a sharp contrast

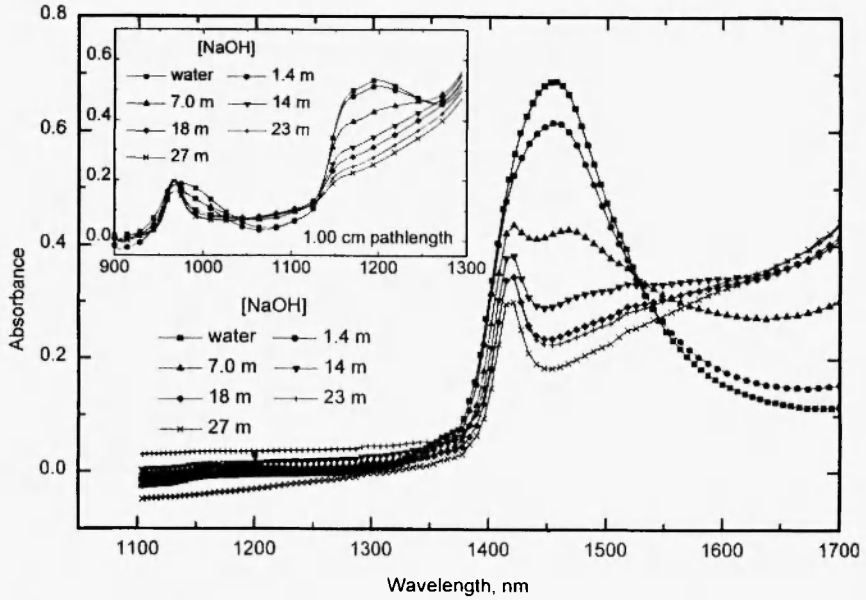

Fig. 1: 1100-1700 nm NIR spectra of NaOH solutions referenced to air; path length, 0.5 mm; 20°C. Inset: 900-1300 nm spectra referenced to air; path length, 1.00 cm.

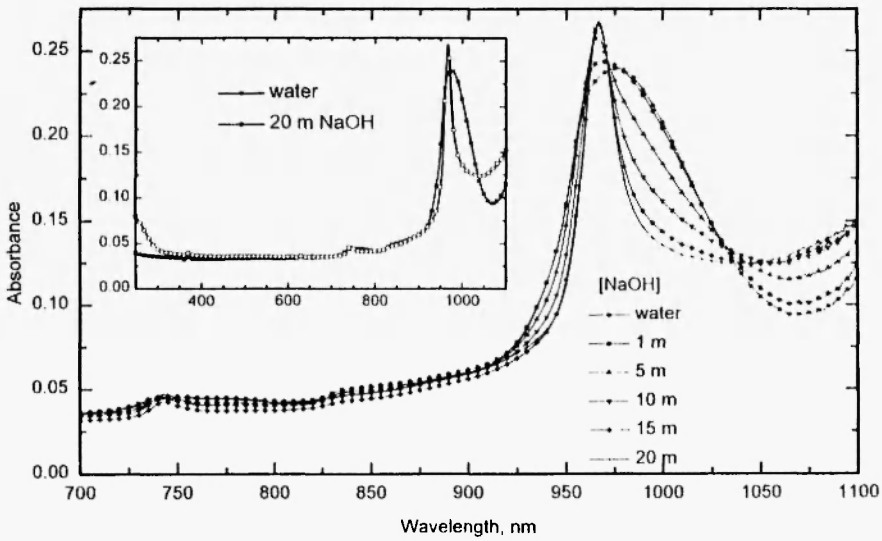

Fig. 2: Short-wave NIR spectra of NaOH solutions referenced to air; path length, 1.00 cm; 20°C. Inset: UV-SW NIR spectra of water and 20 **m** NaOH.

between the pure water and the 20 **m** NaOH absorption spectra in the 250-1100 nm region. Two distinct absorption peaks are evident, a single peak at 976 nm in the pure solvent, and another single peak at 967 nm in the concentrated alkaline solution. In the concentrated solution the majority of the solvent no longer exists in the free (bulk) water state. The 967 nm peak has been previously assigned to the second overtone of the O–H stretching mode /32/. However, as we shall demonstrate with concentrated CsOH and KOH solutions, this peak is not a simple linear function of increasing hydroxide concentration. In NaOH electrolytes, the smooth transition with increasing concentration from the 976 nm to the 967 nm peak is presented in the main portion of Figure 2. As can be seen in the figure, the 967 nm peak continues to increase and to sharpen up to 20 **m** NaOH.

Water activity analysis methodology

In Figures 3 and 4 it is seen that general spectroscopic trends for KOH electrolytes are similar to those observed for NaOH in Figures 1 and 2. However, important differences evidently related to cation association occur in the most concentrated domain, and will be detailed further. Nevertheless, as with the NaOH electrolyte, a broad peak at 1450 nm in pure water is resolved in alkaline solutions into two peaks at 1421 nm and 1457 nm, and, whereas the 1421 nm increases with hydroxide concentration, the 1457 peak diminishes. Similarly, all bands observed in the 1080 to 1250 nm consistently decrease with increasing KOH concentration; while in the 950 to 1050 nm region, two distinct absorption peaks are evident, one single peak at 976 nm appears in the pure solvent. The other single peak at 967 nm is related to the concentrated KOH concentration in which the majority of the solvent no longer exists in the free (bulk) water state.

In each solution studied, and as seen in Figure 4, the absorption peak at 976 nm, which is related to bulk water properties, is strongly correlated to water activity, and can be used to analyze water activity in these solutions. As with NaOH electrolytes, the KOH electrolyte water activities have been extensively characterized /24,25,31/. The inset of Figure 4 presents the dependence of aqueous KOH absorbance at 976 nm, corrected for absorbance at 700 nm (to eliminate gross baseline variation) on the water activity, and provides a precise methodology for the determination of water activity in these solutions. A linear fit of water activity versus wavelength results in an R^2 value of 0.995. Application of the mean absorbance, $A_{mean} = \sum A(\lambda)/\Delta\lambda$,

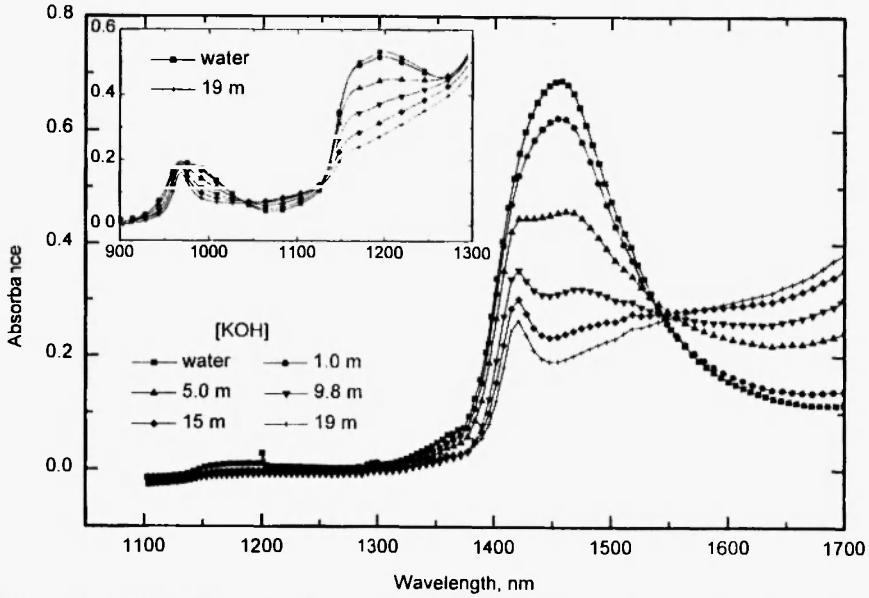

Fig. 3: 1100-1700 nm NIR spectra of KOH solutions referenced to air; path length, 0.5 mm; 20°C. Inset: 900-1300 nm spectra referenced to air; path length, 1.00 cm.

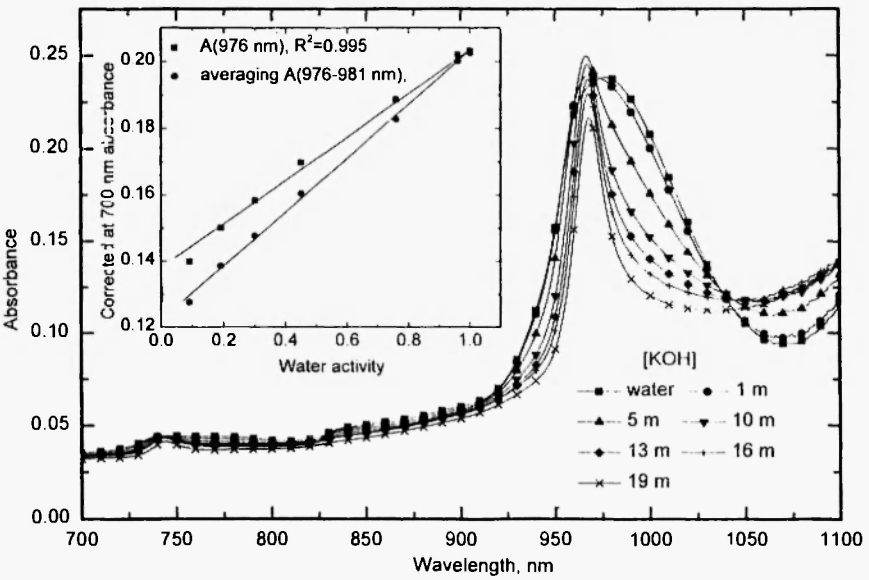

Fig. 4: Short-wave NIR spectra of KOH solutions referenced to air; path length, 1.00 cm; 20°C. Inset: absorbance of KOH solutions corrected at 700 nm on water activity.

over a limited wavelength range ($\Delta\lambda$ = 5 nm) further improves the NIR predictability of water activity, compared to a single wavelength. The range from 976-81 nm provides a best fit for $A_{mean} = 0.2\ a_w$ ($R^2 = 0.998$), and minimizes the influence of the near lying 967 nm hydroxide absorbance.

Figure 5 presents the short-wave length NIR spectra of aqueous LiOH solutions measured under similar conditions up to 5.1 **m**, a concentration approaching LiOH saturation. Due to the limiting maximum solubility of hydroxide in the lithium electrolytes, the OH-related peak at 1421 nm is not observed in these solutions. The behavior of the alkaline spectra in this region is dominated by bulk water, and the larger extinction coefficient of the 1457 nm absorption versus the hydroxide related 1421 nm absorption. As with NaOH and KOH electrolytes, in LiOH electrolytes water activity has also been well characterized, and unlike the NaOH and KOH electrolytes, in approaching the limit of solution saturation does not diminish substantially from unity, i.e., dropping only to $a_w = 0.86$. Increasing solute concentration causes a decrease in a_w. This results in the observed significant drop of 976 nm absorbance, which decreases linearly with increasing NaOH, and KOH solutions. For the smaller maximum decrease of lithium hydroxide electrolyte water activity, due to the smaller upper limit of LiOH solubility, this 976 nm linear relationship between absorbance and water activity is also observed in Figure 6.

Spectral anomalies in Cs and concentrated K aqueous electrolytes

In Figure 6, comparison of the LiOH and CsOH 700-100 nm absorption spectra reveals significant anomalies in the variation of the CsOH spectra with increasing hydroxide concentration. Just like with NaOH in Figure 2, and up through 10 **m** KOH concentrations in Figure 4, with all LiOH solutions, the 967 nm absorption peak increases smoothly with increasing hydroxide concentration. However, in all CsOH electrolytes, unexpectedly, as observed in the inset of Figure 6, the 967 nm peak decreases by a factor of two with increasing hydroxide concentration. This is despite the increasing resolution of the 967 nm peak, as the competing 976 nm again disappears at higher solute concentration. This suppressed absorbance behavior is particularly evident for the CsOH spectra, but is also observed at higher than 13 **m** KOH concentrations in Figure 4. In CsOH and highly concentrated KOH solutions it appears that ion association occurs, as both free hydroxide and bulk water decrease with increasing concentration. It is proposed that,

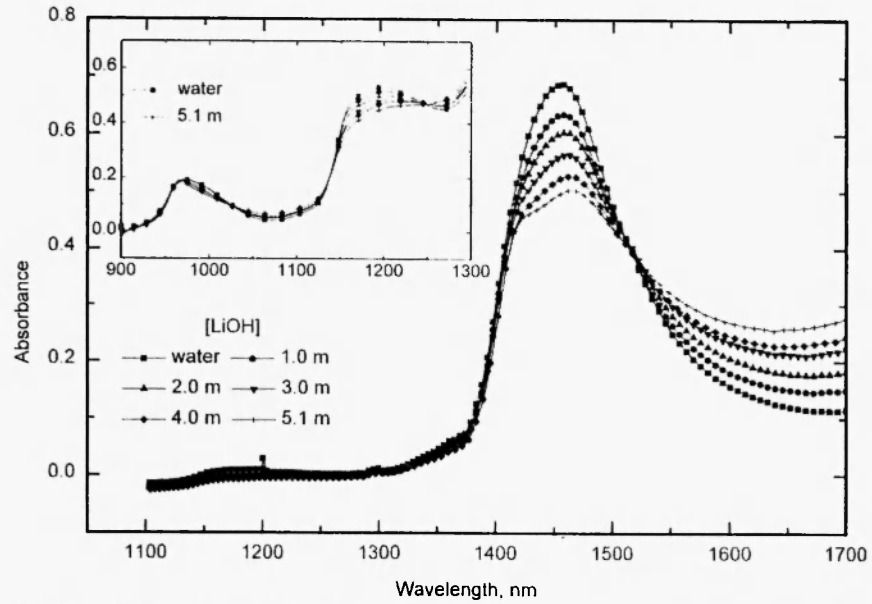

Fig. 5: 1100-1700 nm NIR spectra of LiOH solutions referenced to air; path length, 0.5 mm; 20°C. Inset: 900-1300 nm spectra referenced to air; path length, 1.00 cm.

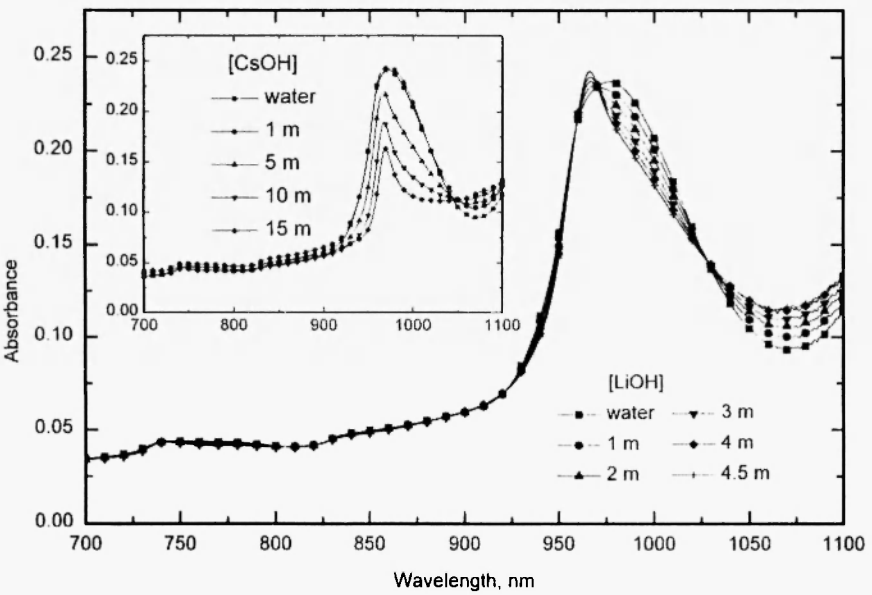

Fig. 6: Short-wave near-infrared (SW NIR, 700-1100 nm) spectra of LiOH solutions referenced to air; path length, 1.00 cm: 20°C. Inset: the same spectra of CsOH solutions.

under these conditions, hydroxide speciation is inhibited as ion association, which may occur with the smaller (less hydrated) cesium and potassium cations. In aqueous solutions containing only monovalent species, Bjerrum and Fuoss ion pairing is generally considered negligible. An alternative model, which has been applied to aqueous alkali hydroxide, acetate and polysulfide solutions, is the localized hydrolysis model initially introduced by Robinson and Harned /33-35/. In this model an additional form of ion pairing occurs in which the anion interacts with protons in the hydration shell of the cation:

$$M^+\cdots H_2O + A^- \rightleftarrows M^+\cdots OH^-\cdots H^+ \qquad (1)$$

Consistent with the observed simultaneous suppression of the 976 and 967 nm peak in the inset of Figure 6, the resulting ion pair on the left of equation 1 will simultaneously diminish both free hydroxide and bulk water concentration. Independent of the appropriate model, it is clear that for CsOH and concentrated KOH solutions, significantly less free chromophore is found in these solutions than in analogous NaOH electrolytes. Interestingly, for CsOH solution absorption in the broader spectral range of 1100 to 1700 nm, and unlike the 950 to 1150 nm range, as presented in Figure 7 the CsOH spectra are similar to those presented and discussed for NaOH and KOH in Figures 1 and 3. With the exception of the 1421 nm absorption, this broader spectral range varies smoothly with bulk water activity. However, in these figures closer inspection of the magnitude of the 1421 nm absorption for the CsOH electrolytes, and the concentrated (13 **m** and higher) KOH electrolytes reveals again that less free hydroxide is available than at comparable NaOH concentrations.

Development of a method for the determination of hydroxide in concentrated solutions.

Determination of hydroxide concentration in caustic solutions is an important industrial and environmental concern. Common methods that are in use today for this purpose are based on pH measurements with low alkali error pH electrode, flow-injection analysis, on-line titration, measurement of conductivity and index of refraction /12/. These techniques require physical invasion of the process with a sampling device, and have not been utilized in

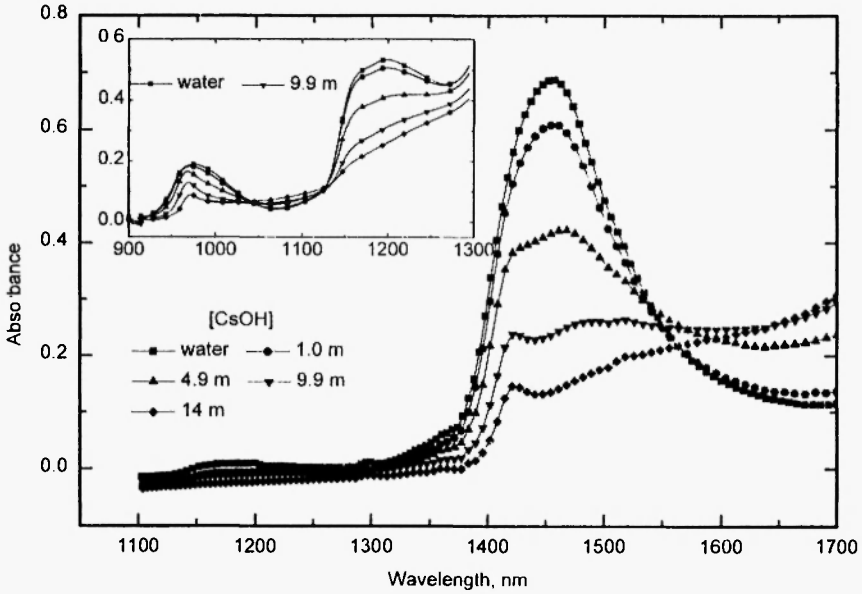

Fig. 7: 1100-1700 nm NIR spectra of CsOH solutions referenced to air; path length, 0.5 mm; 20°C. Inset: 900-1300 nm spectra referenced to air; path length, 1.00 cm.

solutions more concentrated than 5 **m**. Most research pertaining to hydroxide ion spectroscopy has focused on the mid, rather than short wavelength, near infrared spectral regions where strong hydroxide and water absorbance will impair analysis of ultra-concentrated solutions /36-38/. Watson and Baughman /12/ explored near-infrared spectroscopy of hydroxide ion up to concentrations of 2.5 m NaOH in the region 1000 to 2500 nm. Phelan *et al.* /29/ studied hydroxide spectroscopy in the 700-1150 nm spectroscopy of a single alkali hydroxide (up to 5 m NaOH), although no specific effects of ion association were observed.

In the 900-1700 nm range, there are two bands related to the first overtone of free hydroxide stretching at 1421 nm and the first and the second overtones at 967 nm. In the above range these peaks can be utilized in the specific analysis of hydroxide concentration, when discriminated from the other bulk water correlated bands in this region. However, both the 967 and 1421 nm absorptions are located close to, and are perturbed by, the bulk water bands at 976 and 1457 nm. This is one of several reasons that simple NIR absorbance analysis of hydroxide is problematic. In addition to the

variation of solvent baseline due to constraints on bulk water, an additional challenge is the significant experimental variation in the spectral baseline which frequently occurs in concentrated solutions due to an increase in solution viscosity. Viscous solutions tend to retain suspended materials including air bubbles, which cause baseline shifts. A third challenge to the analysis of highly concentrated solutions is related to an increase in the index of refraction, n, for increasing concentration. Absorbance is influenced by refractive coefficient n of the sample /28/:

$$A = \varepsilon\, l\, n / (n^2 = 2)^2 \qquad (2)$$

As an example, the index of refraction increases from n = 1.33 in pure water to n = 1.34 in 1 **m** KOH, to n = 1.40 in 10 **m** KOH. In accordance with eq. 2, this will cause a small, but significant, decrease of 4% in absorbance in the concentration range 1 to 10 **m** KOH.

Figure 8 presents the second-order derivative analysis, $\partial^2 A(\lambda)/\partial\lambda^2$ in the 900 to 1000 nm region, of the NaOH spectra presented in Figure 1, and

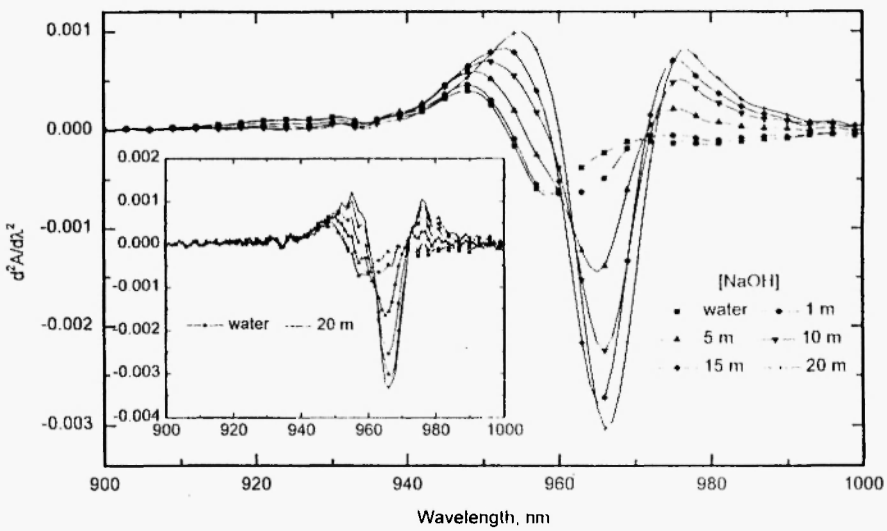

Fig. 8: Inset: Second-order derivative analysis, $\partial^2 A(\lambda)/\partial\lambda^2$, of the aqueous NaOH spectra presented in Figure 2. In the main portion of the figure, the $\partial^2 A(\lambda)/\partial\lambda^2$ spectra were obtained from the same data by use of the Savitsky-Golay Algorithm with a filter length of 7 and second-order polynomial.

provides improved discrimination of closely situated absorption peaks. This analysis provides a sensitive analysis of the 967 nm hydroxide peak, despite the fact that the water related peak lies within 9 nm. This second-order derivative analysis also removes linear baseline effects, and diminishes the impact of slowly varying nonlinear baseline effects, as caused by index of refraction variation. These improvements considerably improve the resolution of the hydroxide peak; however, as seen in the inset of Figure 8, one disadvantage of the differential process is a decrease of the signal-to-noise ratio (S/N) compared to the simple absorbance spectra in Figure 1. Signal-to-noise ratio of a differential process can be improved by proper choice of a derivatization algorithm, i.e., by means of a Savitsky-Golay algorithm with a suitable polynomial degree and filter length. The data in the main portion of Figure 8 were obtained by use of a Savitsky-Golay algorithm with a filter length of 7 and a second order polynomial. A similar second-order derivative analysis, $\partial^2 A(\lambda)/\partial\lambda^2$ of the spectra in the 1300 to 1500 nm was also performed. As seen in Figure 9, both 967 and 1421 nm $\partial^2 A(\lambda)/\partial\lambda^2$ analyses exhibit a simple linear dependence over a wide hydroxide concentration range, in a variety of alkaline hydroxide solutions.

Figure 9 summarizes the second-order derivative analysis of several LiOH, NaOH KOH and CsOH electrolytes, determined as exemplified for NaOH in Figure 8, in each case only up to a limited maximum concentration. Concentrated solutions generally are reported in molal (mass based), rather than molar (volume based) units to probe thermodynamic activities, and molal concentration units are used throughout this study. However, chromophore concentrations vary with volume, and converted molar units are also useful for analytical methodology. Hence, the left-hand side of Figure 9 reports the variation of $\partial^2 A/\partial\lambda^2$ with moles hydroxide per kg water (**m**, molality), whereas in the right-hand figure inset it is reported versus simple molar units (**M**, moles hydroxide per liter solution). With either unit, as is evident from the highly linear dependence observed in the figure, this second-order derivative analysis, both at 967 and 1421 nm, is widely applicable and depends only on molal or molar OH^- concentration. For example, a similar linear dependence of $\partial^2 A$ (λ = 1411 nm)$/\partial\lambda^2$ on hydroxide concentration was observed for all LiOH solutions up to saturation concentrations, and for up to 18 **m** NaOH, or up to 13 **m** KOH or 10 **m** CsOH, respectively. At 1421 nm, a single value of the second-order derivative "extinction coefficient" of -8.0×10^{-5} cm^{-1} $\mathbf{M}^{-1}$ predicts hydroxide concentration for each of these highly LiOH, NaOH, KOH, and CsOH solutions

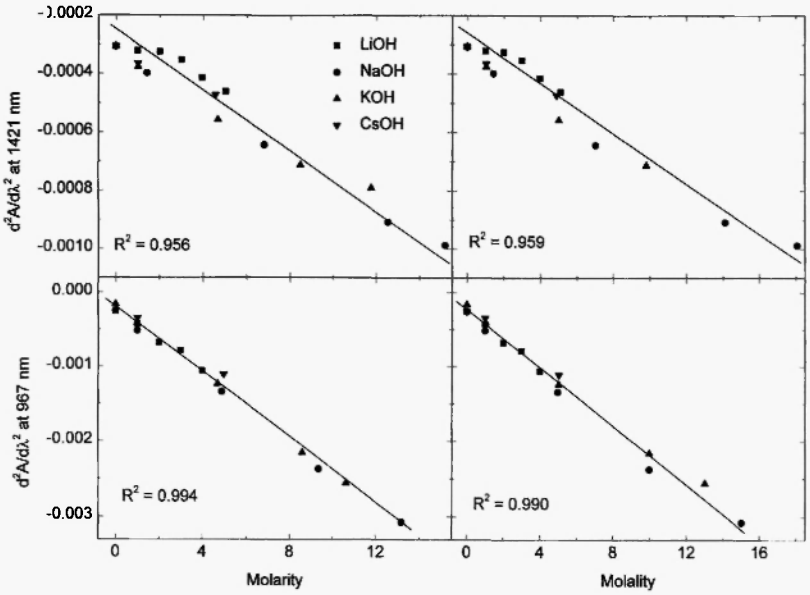

Fig. 9: Molal or molar hydroxide concentration second-order derivative analysis of a variety of alkali hydroxide electrytes are calculated from $\partial^2 A(\lambda)/\partial\lambda^2$ using the data in Figures 1-7.

with a correlation coefficient, R^2 = 0.959. As with the 1421 nm second derivative analysis, a single value of the second-order derivative "extinction coefficient" of -2.5×10^{-4} cm^{-1} $\mathbf{M}^{-1}$ predicts the hydroxide concentration at 967 nm for each of the highly concentrated LiOH, NaOH, KOH, and CsOH solutions indicated in the left-hand Figure 9 inset. A linear fit of the data for the indicated solutions in the figure inset provides a correlation coefficient, R^2 = 0.994 as applied to all indicated hydroxide electrolytes. Finally, the linear relationship observed in Figure 9 between $\partial^2 A/\partial\lambda^2$ and hydroxide concentration does not apply in the highest concentration domain, and in each case $\partial^2 A/\partial\lambda^2$ is smaller than expected. This is observed for NaOH concentrations of 18 **m** and higher, and is similarly observed at KOH or CsOH concentrations above 13 **m** and 10**m**, respectively. In these highest concentration domains, as previously discussed, ion association can diminish absorption, and hence also diminish $\partial^2 A/\partial\lambda^2$. Therefore, the second-order derivative methodology is not applicable due to these highest concentration domains.

Interferences to hydroxide analysis

To probe the influence of several commonly occurring and potentially interfering species on the spectra of alkaline solutions, two sets of sample solutions were prepared. In solutions containing up to 10 **m** KOH or 10 **m** NaOH, a variety of salts at 1 **m** concentration were added. A second-order derivative analysis was performed at 967 nm. The hydroxide concentration was calculated by use of a second-order derivative analysis at 967 nm in the solutions without the added salt, based on the second-order derivative "extinction coefficient" reported in the previous section. As also seen in Table 1, analysis based on a calculation of the mean average value of the second-order derivative in the range 966-71 nm improves results. As can be seen from Table 1, only acetate salts cause a significant deviation from the expected hydroxide concentration. Other salts, including nitrates, nitrites, thiocyanate, which can be present in the solutions in very high concentrations, did not significantly interfere with the results of the analysis. Additional salts, not shown in Table 1, such as sulfates, have only a limited solubility in concentrated alkaline solutions. The small, but significant, effect

Table 1

Influence of various dissolved salts on hydroxide determination. Interference by a 1 m concentration on 10 m hydroxide is shown. Hydroxide concentration is determined by the second-order derivative analysis described in the text at 967 nm, or at a mean analysis over 966-71 nm.

Solution	% deviation from NaOH concentration		% deviation from KOH concentration	
	967 nm	966-71 nm	967 nm	966-71 nm
MOH and CH_3COOK	-9.2	-8.8	-8.7	-8.4
MOH and CH_3COONa	-5.4	-4.8	-7.5	-7.2
MOH and CH_3COOLi	-	-	-11.0	-10.1
MOH and KNO_3	-1.9	-1.2	1.2	1.5
MOH and KNO_2	-2.8	-2.2	-2.1	-1.9
MOH and $NaNO_2$	-2.0	-1.3	-1.3	-1.1
MOH and KSCN	-5.6	-4.9	-4.4	-3.9
MOH and NaSCN	-5.1	-4.2	-3.1	-2.7

of acetates on the hydroxide absorbance may be due to the related ion association behavior of aqueous acetate and hydroxide anion activities in these solutions /10/.

CONCLUSIONS

NIR spectroscopy represents an effective method of spectrochemical analysis of concentrated solutions, provided that all the notable features of this technique are recognized and controlled. These features include the relative height of the solvent compared to solute absorbances, the changing nature of this solvent absorbance in the concentrated solute domain, proper choice of analyte absorption based on understanding of processes occurring in the analyte solution, and careful assignment of the spectroscopic bands.

It is shown that analyte strongly affects the conventional aqueous baseline of these measurements, and this baseline behavior must be addressed for effective NIR analysis. In the domain of molar analyte concentration, the water baseline changes drastically as solute interacts and confines bulk solvent. After controlling these notable features, near-infrared analysis provides a powerful tool for the analysis of concentrated solutions, as exemplified by alkaline solutions, and enables determination of a wide range of hydroxide concentration and water activity. Hydroxide analysis is based on the second-order derivative of solution absorbance at967 nm or 1421 nm, $\partial^2 A(\lambda)/\partial\lambda^2$, which provides a precise methodology for hydroxide determination in concentrated Li, Na, K electrolytes. An unexpected observed decrease in A (λ = 967nm) in solutions with concentrations higher than 13 **m** KOH and in CsOH solutions is consistent with ion-association. Addition of a variety of 1 **m** salts does not significantly interfere with the hydroxide analysis at 967 nm, with the exception of acetate salts, which cause a deviation of 10% in a 10 **m** KOH or NaOH electrolyte. A linear correlation between water activity of the solutions and 976 nm absorbance was observed with a path length normalized maximum absorbance of A (λ = 976 nm) = 0.24 cm^{-1} occurring in pure water.

ACKNOWLEDGMENT

The authors are grateful to Professor Efrat Liphshitz, Mr. Ilya Litvin and Dr. Horia Porteanu for the facilities and support in the long wavelength NIR measurement. This project was supported in part by the General Motors Foundation, the Joint German-Israeli Research Program BMBF, and the Technion's VPR and Promotion of Research Funds.

REFERENCES

1. K. Liu, M.G. Brown, C. Carter, R.J. Saykally, J.K. Gregory and D.C. Clary, *Nature*, **381**, 501 (1996).
2. S.W. Benson and E.D. Siebert, *J. Am. Chem. Soc.*, **114**, 4269 (1992).
3. J.K. Gregory and D.C. Clary, *J. Phys. Chem.*, **100**, 18014 (1996).
4. J.K. Gregory, D.C. Clary, K. Liu, M.G. Brown and R.J. Saykally, *Science*, **275**, 814 (1997).
5. L.X. Dang and T. Chang, *J. Chem. Phys.*, **106**, 9149 (1997).
6. K. Buijs and G.R. Choppin, *J. Chem. Phys.*, **39**, 2035 (1963).
7. D.F. Horning, *J. Chem. Phys.*, **40**, 3119 (1964).
8. G.R. Choppin and M.R. Violante, *J. Chem. Phys.*, **56**, 5890 (1972); *ibid*, 5899.
9. J.G. Bayly, V.B. Kartha and W.H. Stevens, *Infrared Phys.*, **3**, 211 (1963).
10. T. Hirschfeld, *Appl. Spectrosc.*, **39**, 740 (1985).
11. J. Lin and C.W. Brown, *Trends Anal. Chem.*, **13**, 320 (1994).
12. E. Watson, Jr. and E.H. Baughman, *Spectroscopy*, **2**, 44 (1987).
13. A. Grant, A. Davies and T. Bilverstone, *Analysis*, **1141**, 819 (1989).
14. C.J. Thompson, J.D.S. Danielson and L.B. Callis, *Anal. Chem.*, **69**, 25 (1997).
15. S.J. Choquette, S.N. Chelser, D.L. Duewer, S. Wang and T.C. O'Haver, *Anal. Chem.*, **68**, 3525 (1996).
16. M.K. Alam and J.B. Callis, *Anal. Chem.*, **66**, 2293 (1994).
17. A. Fong and G.M. Hieftje, *Anal. Chem.*, **67**, 1139 (1995).
18. S.M. Donahue, C.W. Brown, B. Caputo and M.D. Modell, *Anal. Chem.*, **60**, 1873 (1988).
19. P. Robert, D. Bertrand, M. F. Devaux and A. Sire, *Anal. Chem.*, **64**, 664 (1992).

20. W.H.A.M. van den Broek, D. Wienke, W.J. Melssen, C.W.A. de Crom and L. Buydens, *Anal. Chem.*, **67**, 3753 (1995).
21. S. Licht and F. Fourouzan, *Anal. Chem.*, **64**, 2003 (1992).
22. S. Licht, K. Longo, D. Peramunage and F. Fourouzan, *J. Electroanal. Chem.*, **318**, 111 (1991).
23. S. Licht, F. Fourouzan and K. Longo, *Anal. Chem.*, **62**, 1356 (1990).
24. D. Peramunage, F. Fourouzan and S. Licht, *Anal. Chem.*, **66**, 378 (1994).
25. S. Licht, *Anal. Chem.*, **57**, 514 (1985).
26. S. Licht, "Electrochemical and chemical analysis in highly concentrated solutions", in: *Electroanalytical Chemistry*, A. Bard and I. Rubinstein (Eds.), Marcel Dekker, 1988; Vol. 20, 87.
27. H.J. Kim, *J. Chem. Phys.*, **105**, 6833 (1996).
28. G. Kortum and M. Seiler, *Angew. Chem.*, **48**, 687 (1939).
29. M.K. Phelan, C.H. Barlow, J.J. Kelly, T.M. Jinguji and J.B. Callis, *Anal. Chem.*, **61**, 1419 (1989).
30. J. Paquette and C. Jolicouer, *J. Solution Chem.*, **6**, 403 (1977).
31. B.E. Conway, *Electrochemical Data*, Elsevier Publishing Company, London; 1952.
32. O.H. Wheeler, *Chem. Rev.*, **59**, 642 (1959).
33. J. O'M. Bockris, *Modern Electrochemistry*, Plenum Press, New York, 1970; p. 260.
34. R.A. Robinson and H.S. Harned, *Chem. Rev.*, **28**, 419 (1941).
35. S. Licht, R. Tenne, H. Flaisher and J. Manassen, *J. Electrochem. Soc.*, **133**, 52 (1986).
36. R.M. Diamond, *J. Am. Chem. Soc.*, **80**, 4808 (1958).
37. D.A. Giguere, *Rev. Chim. Miner.*, **20**, 588 (1983).
38. W.R. Busing and D.F. Horning, *J. Phys. Chem.*, **65**, 284 (1961).
39. M. Moskovits and K.H. Michelian, *J. Am. Chem. Soc.*, **102**, 2207 (1980).